Label-free electrochemical detection of Cloxacillin antibiotic in milk samples based on Molecularly Imprinted Polymer and graphene oxide-gold nanocomposite

Article *in* Measurement · May 2019

DOI: 10.1016/j.measurement.2019.05.068

CITATIONS
4

READS
166

5 authors, including:

Saeid Jafari
Islamic Azad University of Yazd
6 PUBLICATIONS **36** CITATIONS
SEE PROFILE

Mohammad Dehghani
Islamic Azad University of Yazd
11 PUBLICATIONS **91** CITATIONS
SEE PROFILE

Navid Nasirizadeh
Islamic Azad University of Yazd
96 PUBLICATIONS **2,061** CITATIONS
SEE PROFILE

Mohammad Hadi Baghersad
Baqiyatallah University of Medical Sciences
14 PUBLICATIONS **182** CITATIONS
SEE PROFILE

Measurement 145 (2019) 22–29

Contents lists available at ScienceDirect

Measurement

journal homepage: www.elsevier.com/locate/measurement

Label-free electrochemical detection of Cloxacillin antibiotic in milk samples based on molecularly imprinted polymer and graphene oxide-gold nanocomposite

Saeid Jafari [a], Mohammad Dehghani [a], Navid Nasirizadeh [b,*], Mohammad Hadi Baghersad [c,*], Mostafa Azimzadeh [d,e,f]

[a] Young Researcher and Elite Club, Yazd Branch, Islamic Azad University, Yazd, Iran
[b] Department of Textile and Polymer Engineering, Yazd Branch, Islamic Azad University, Yazd, Iran
[c] Applied Biotechnology Research Center, Baqiyatallah University of Medical Sciences, Tehran, Iran
[d] Medical Nanotechnology & Tissue Engineering Research Center, Yazd Reproductive Sciences Institute, Shahid Sadoughi University of Medical Sciences, PO Box: 89195-999, Yazd, Iran
[e] Stem Cell Biology Research Center, Yazd Reproductive Sciences Institute, Shahid Sadoughi University of Medical Sciences, PO Box: 89195-999, Yazd, Iran
[f] Department of Advanced Medical Sciences and Technologies, School of Paramedicine, Shahid Sadoughi University of Medical Sciences, Yazd 8916188635, Iran

ARTICLE INFO

Article history:
Received 25 February 2019
Received in revised form 19 May 2019
Accepted 21 May 2019
Available online 27 May 2019

Keywords:
Molecularly imprinted polymer
Electrochemical
Cloxacillin
Graphene oxide
Gold nanoparticle

ABSTRACT

Detection of applied antibiotics in food productions could be the first step to avoid future health consequences. The aim of this work was to the synthesis of molecularly imprinted polymer (MIP) particles via non-covalent procedure and evaluation of efficiency MIP for the selective collection of Cloxacillin (CLO) from aqueous and biological samples and consequently quantification of separated CLO using an electrochemical nanosensor. The effect of operational parameters including pH, contact time and MIP dosage for optimization of CLO collection condition were studied. The CLO quantities were determined by a developed electrochemical nanosensor based on a screen-printed electrode modified with graphene oxide and gold nanoparticles. The results showed that the optimum conditions for removal of CLO (92%) were determined at pH = 8.5, with 89 min as contact time and 0.79 g MIP. The linear range was from 110 to 750 nM and the detection limit of the nanosensor was 36 nM. The performance of the MIP-based nanosensor for the spiked Cloxacillin detection in real milk samples showed the potential of the developed nanosensor to be considered in future real sample measurement analysis.

1. Introduction

The growing rate of antibiotic usage in modern animal husbandry, especially with excessive dosage, is a new threat for human health as a food product user, due to the remaining of antibiotics in the animal products such as meat, milk, etc. Therefore, there is a need for an efficient system to determine/quantify these compounds from the food samples or even environment such as wastewater [1–3].

Cloxacillin (CLO) is a type of beta-lactamase-resistant penicillin. This antibiotic is used to treat infections caused by Staphylococcus species, microbial infections with golden staphylose (a bacterium producing penicillinase), skin infections, and respiratory system. CLO has oral absorption, but its absorption is reduced taking it with food. More than 50% of the CLO is absorbed by the oral route and its concentration reaches its peak after 1–2 h. The half-life of the drug is between 1 up to 5 h, which increases by up to 2.5 h due to poor kidney function. About 30–60% of unchanged CLO is usually excreted by the kidney [4,5].

Various methods such as adsorption with activated carbon [6], reverse osmosis [7], biological methods [8], as well as advanced oxidation processes include ozonation [9], photo Fenton [10], sono-oxidation [11], ultrasound radiation [12], ultraviolet radiation [13] has been used to remove/collect drug compounds from various samples. In this way, the adsorption process have been used for a variety of new materials available for the recovery process [14]. Researchers synthesis and design a suitable adsorbent, not only having the ability to absorb compounds, but have high absorption capacity as well as being stable in basic and acidic environments [15–19].

Nowadays, a new generation of polymeric absorbers with unique properties is used by researchers to reducing compounds

* Corresponding authors.
E-mail addresses: nasirizadeh@iauyazd.ac.ir (N. Nasirizadeh), hadibaghersad@bmsu.ac.ir (M.H. Baghersad).

https://doi.org/10.1016/j.measurement.2019.05.068
0263-2241/

in aqueous. It could be to mention the diverse characteristics of these adsorbents, including selective absorption, high absorption capacity, high specific surface, chemical, thermal and mechanical stability, and the reusing ability, in addition capability of using in aqueous and petroleum media. Molecularly imprinted polymers (MIPs) are polymeric particles contain selective identification sites relative to template molecule, which have attracted researchers in the last decade. During the imprinting process, template molecules are placed in the 3D polymer network based on shape, size and orientation functional groups [20–22].

To best of our knowledge, few attempts have yet been made to regarding the synthesis of MIP for antibiotic CLO and its application for remove/collect of CLO from aqueous and biological media. Nevertheless, in the study performed by Ashley et al., [23], the MIP prepared with CLO was applied for extraction and determination of CLO using Surface-Enhanced Raman Spectroscopy Nanopillars and on the other hand, Du et al. [24] describes the application of molecularly imprinted sol–gel material as adsorbents to the extraction of CLO and recognition of cloxacilloic acid towards CLO.

On the other hand, there are few studies regarding electrochemical detection of CLO in food samples. Electrochemical methods, in comparison with other analytical methods, do poses some advantages such as high sensitivity, the need of small amount of sample, low-cost and less complicated methods [25–28]. Furthermore, the application of nanomaterials and nanocomposites in electrochemical detection methods bring higher sensitivity and conductivity and enhances the function of the sensing mechanism [29–31]. In this way graphene derivatives, such as graphene [32], graphene oxide [33] and reduced graphene oxide [29], have been used before in electroanalytical methods for their electron transfer enhancement, providing a media for other molecules/nanoparticles to attach and increase the surface area of the electrode. Gold nanoparticles (AuNPs) will also provide the same advantages along with a surface that could be used for electrocatalytic activity [34–37]

The present study describes for the first time the application of a MIP imprinted with CLO antibiotic to the direct detection of CLO from aqueous and milk sample using the pre-concentrate technique. The selective MIP particles are synthesized by mass polymerization in the presence of a template molecule to forming the MIP. Subsequently, an electrochemical nanosensor for quantification of CLO was developed based on a screen-printed carbon electrode (SPCE) modified with the MIP/graphene oxide (GO)/gold nanoparticles nanocomposite.

2. Experimental

2.1. Materials and instruments

Cloxacillin antibiotic (CLO) (98%) (See Sup. Fig. 1) as template and 2, 2′-Azobis (2-methylpropionitrile) (AIBN) as initiator of polymerization, as well as Graphene oxide (GO) (catalog number 763705) and Gold nanoparticles (AuNPs) (average diameter 30 nm, catalog number 753629) were purchased from Sigma-Aldrich Co. (USA) Ethylene glycol di-methylacrylate (EGDMA) as cross-linker and Methacrylic acid (MAA) as monomer was obtained from Merck Co. (Germany). The buffer phosphate solution as carrier electrolyte was prepared using 0.1 M H_3PO_4 and NaOH.

For assessing of MIP performance in removal of CLO from aqueous, CLO residues was determined using galvanostat/potentiostat M101 Autolab (Metrohm, Netherland) attached to NOVA software and Screen-printed carbon electrode (SPCE, model DRP-C110 from DropSens Co., Spain). The Field Emission Scanning Electron Microscopy (FESEM) and transmission electron microscopy (TEM) studies used a TESCAN model MIRA3 FESEM and Carl Zeiss LEO 906 TEM, respectively. The CLO was extracted from MAA/EGDMA copolymer matrix using soxhlet extractor (Germany).

2.2. Preparation of MIP

The CLO Molecularly imprinted polymer was prepared via the following procedure which is a slight modification of the previous protocol [38]. Amount of 9.0 mg CLO as a template, 35.0 mL dry chloroform and 0.3 mL MAA was added to 100 mL balloon-flask and stirred for 15 min. Afterward, 20.0 mL EGDMA as cross-linker was added to the flask, then CLO and MAA were dissolved in chloroform (35.0 mL), and the resulting mixture was stirred for 15 min and then stood for another 4 h to prepare the pre-assembly solution. Then, EGDMA and AIBN (initiator, 0.22 g) was dissolved in the pre-assembly solution. The mixture was sealed and deoxygenated with a stream of nitrogen. The obtained pre-polymerization solution was shaken and stirred at 65 °C for 24 h. At the end of the reaction, the polymers were separated from the reaction medium.

Following, the polymers were extracted with MeOH in soxhlex extractor to remove CLO until no CLO was detected by the electrochemical determination in extraction solutions and washed with MeOH for 24 h. Then, the wet polymers were dried at 60 °C in a vacuum oven for 24 h. The resulting MIP was used in adsorption tests for separation of CLO from aqueous media. As a control experiment, non-imprinted polymer (NIP) particles were also prepared in a similar procedure but without the addition of CLO.

2.3. Experiments of CLO collection performance

The operational parameters include contact time of MIP as adsorbent, pH and used MIP amount was affected on the removal efficiency of CLO. In this research, removal conditions of CLO were optimized using response surface method (RSM) by changing of contact time, pH and MIP dosage. The RSM consists of a group of statistical and mathematical methods that allow the optimal conditions to be achieved in complex systems. For the study, the composite statistical design (CCD) was used; this model is a combination of second-order (quadratic) functions and interaction coefficients.

Supplementary Table 1 lists the variables and their intervals. By the introduction of intervals the mentioned parameters to the Design-Expert software, twenty tests were designed based on the CCD (Supplementary Table 2). The CLO removal tests were performed out by following way: the identified amount of MIP was added to a solution containing 0.05 g/L CLO (its pH was adjusted by PBS according to each test listed in Table 2). The mixture was gently stirred for about 10–15 min and then the residual amount of the CLO concentration in solution is determined by differential pulse voltammetry.

In addition, the textural features of the synthesized MIP were assessed using N_2 adsorption/desorption isotherms at 77 K using a Belsorp analyzer (BEL Japan Inc). The specific surface area (S_{BET}) was calculated by Brunauer–Emmett–Teller (BET) gas adsorption method and the pore size distribution was obtained by means of Barrett–Joyner– Halenda (BJH) method. The thermogravimetric analysis was performed in a N_2 atmosphere at a heating rate of 10 °C min-1 from room temperature to 800 °C using A Perkin Elmer TGA 4000 (USA).

2.4. Determination of adsorption capacity of MIP and residues CLO content

The absorption capacity of the MIP for CLO is determined from the following equation (Eq. (1)) reported in a previous publication [39]:

$$q_e = \frac{(C_i - C_f) \times V}{m} \quad (1)$$

where, q is absorption capacity (mg/g), V is volume solution (L), Ci and C_f are initial and final CLO concentration in the sample (mg/L) and m is mass of MIP (g). The CLO collection percentage from aqueous was determined by below equation reported in a previous publication [39]:

$$\text{Collection } (\%) = (1 - C_f - C_i) * 100 \quad (2)$$

2.5. Determination of CLO using nanosensor

The CLO concentration in solution is determined by the electrochemical method using screen-printed carbon electrode (SPCE) modified with gold nanoparticles and graphene oxide. The modification steps of SPCE as a sensor for determination of CLO as follows. Firstly, a drop containing 2.0 µL of the GO solution (2.0 mg mL^{-1}) was dropped on the surface of the bare SPCE and then the electrode was later kept in an isolating container until it was completely dried. Afterward, a drop of AuNPs dispersion (final concentration of 25.0 mg mL^{-1}) was placed on the GO-modified SPCE and the electrode was kept in the sealed and humid container to be slowly dried. The Differential pulse voltammetry (DPV) analysis was performed in the 0.1 M phosphate buffer solution (pH 7.0) in the range of 0.1–1.0 V.

3. Results and discussion

Scheme 1 is representing the process of MIP formation (Section A), collecting/pre-concentration of CLP molecules using MIP (Section B) and fabrication process of the electrochemical nanosensor for CLP quantification (Section C) that is explained earlier in the experimental section.

3.1. Optimization and characterization of MIP

The response surface graphs are designed to show and estimate the efficiency of the effective factors in the CLO absorption on MIP by applying non-dependent variables, as shown in Sup Fig. 2. These graphs show the effect of interactions between the two factors from the three factors investigated on the efficiency of CLO remove from the solution, while the other variables are constant. The Sup Fig. 2a shows the effect of simultaneous changes in the contact time (1–120 min) and the amount of MIP (0.01–1.0 g) on the collection percentage of CLO, when pH was equal to 7.92. It can be seen, by increasing the contact time of MIP in a CLO solution up to 90 min, the CLO removal efficiency increases. The prolonging of the contact time of MIP in the solution has no significant effect on the removal efficiency of CLO.

Adsorbent mass is one of the important factors in removing contaminants by adsorption. If this amount is less than the required amount, the absorption step may not be complete and all of the analyte will not be adsorbed by the sorbent. In this study, with the increase in the amount of MIP particles, which is used as an adsorbent to remove CLO, the removal efficiency has increased. Due to the fact that the number of CLO molecules is constant in the solution, and by increasing the number of active sites for the adsorption of CLO molecules, it is possible to improve the CLO removal process by increasing the amount of MIPs. Similar results have been reported about increasing the amount of ampicillin removal by MIPs [18].

The Sup Fig. 2b shows the effect of simultaneous changes in pH (3–10) and contact time on the removal percentage of CLO while a MIP value is 0.68 g. It is observed that with increasing pH from 3 to 7, the CLO removal rate with a rather steep slope increased and then decreased in the range of 7 to 10.

The pH of the solution is one of the affecting factors on chemical surface properties of the adsorbent, in other words, the surface

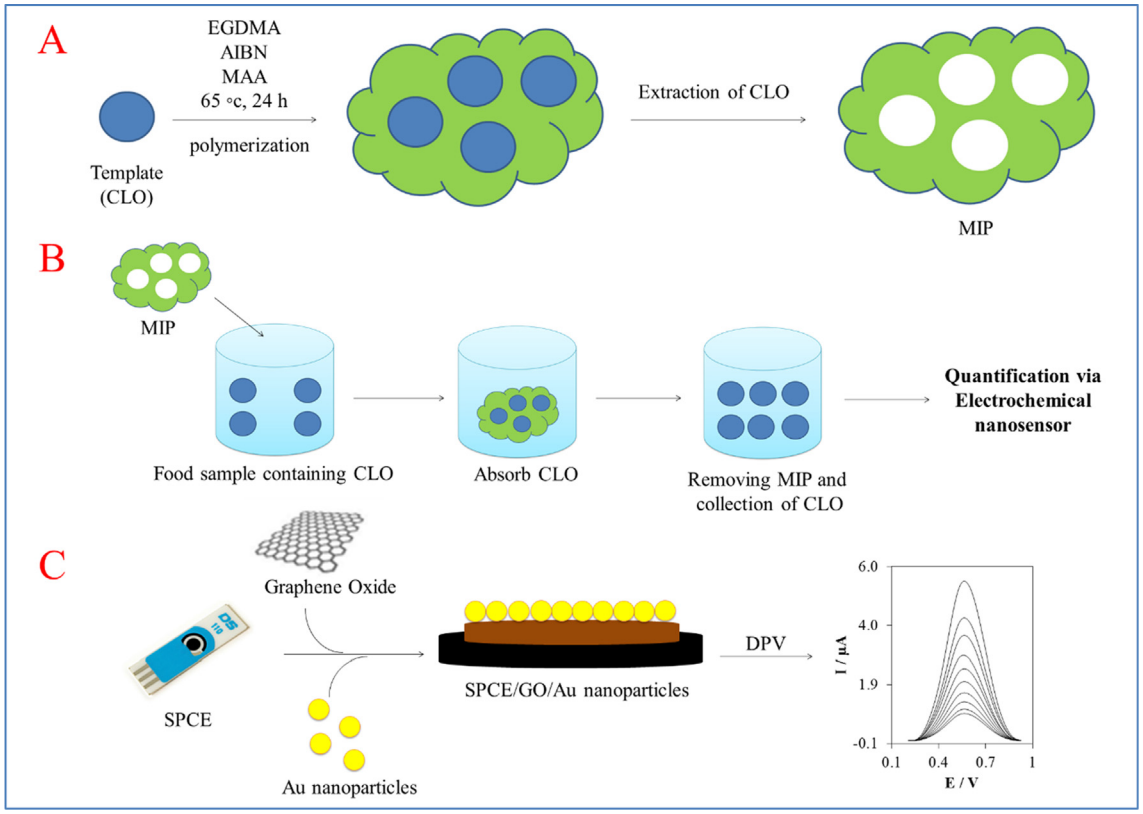

Scheme 1. Representation of the MIP fabrication, pre-concentration and detection of the CLO using the electrochemical nanosensor.

charge of absorbent may be varied in acid or alkaline conditions. By reviewing literature, it can be abundantly found that pKa of MAA, which is the main body of the polymer, is reported to be about 4.65. This means that the functional groups of COOH are converted to $COOH_2^+$ in acidic environments (>4.65) and have a positive partial charge [19]. While CLO is also positive in acidic environments, repulsive positive charges interfere with the interaction between the CLO functional groups and the carbonyl groups of MAA, as a result, a less amount of CLO will be adsorbed by the MIP. On the other hand, in the mildly acidic environment (4.65 <) to neutral, the COOH converts to COO^-, that is, a negative species in the environment, therefore, conditions are appropriate for interactions between CLO and MIP particles, consequently, the highest remove is observed in the neutral region. With increasing pH, electrostatic repulsion between CLO and functional groups at the MIP surface also increased, resulting in fewer amounts of CLO will adsorbs on MIP. What can be learned from the results of the effect of contact time is that the rate of CLO absorption on the MIP particles is slowly, so that the balance time is observed in 90 min. It seems that CLO molecules have saturated MIP surface over time, and it can be said that the adsorption process has reached a balance. On the other hand, with the increase in the MIP amount in solution, the removal efficiency of CLO is gradually increased.

In the adsorption process, there are ion exchange site and specific proprietary positions on the adsorbent surface, where the antibiotic will interacts to them. The prolonging times, there will be enough time for interaction of antibiotic molecules with specific absorption sites. On the other hand, the prolonging the contact time after reaching the equilibrium caused to some of the adsorbed molecules on MIP with weak interaction exits from its place and replaced by another molecule. Thus, we have seen no significant change in efficiency. Similar studies have been carried out using different adsorbents on antibiotic removal, where these conducted to investigate the contact time and the amount of adsorbent.

Du et al. have been used modified silica gel particles for removal of cloxacillin. It has been reported that the equilibrium time for antibiotic absorption on these particles is about 2 h [24]. In another study, kaolin was used to the elimination of tetracycline, where a balance time of about 5 h has been reported [40]. By comparing the equilibrium times, we can conclude that the highest removal efficiency shorter time using proposed adsorbent is obtained than similar ones.

The morphology of prepared polymer particles in presences (MIP) and absence (NIP) of CLO molecules (as a template) was observed by field emission scanning electron microscopy. Due to the trapping of the CLO molecules in MAA molecular chains during bulk polymerization and their extraction by the solvent in soxhelt extractor, numerous cavities are observed at the polymer surface (Fig. 1A). But, Fig. 1b shows the particle morphology of the NIP prepared from MAA/EGDMA. As shown, we can see a smoother structure than the MIP due to no CLO adding to the mixture of MAA/EGDMA during bulk polymerization.

In this study, during the synthesis of NIP (polymer without molecular imprint), due to the absence of the (CLO) molecule at polymerization process, it forms a continuous structure with less porosity than MIP. However, in the SEM image of the MIP, there is an enormous number of pores. This was due to the formation of a polymer network around the template molecule, which these pores created during the extraction process of CLO and its remove from the polymer matrix. The presence of these pores can help to increase the effective surface area for contacting the polymer surface with the CLO molecule and thus separating it from the solution.

The optimum conditions for the removal of CLO were obtained in pH 8.5, the contact time of 89 min, and 0.79 g MIP. The absorption capacity of both synthesized polymers of MIP and NIP for CLO

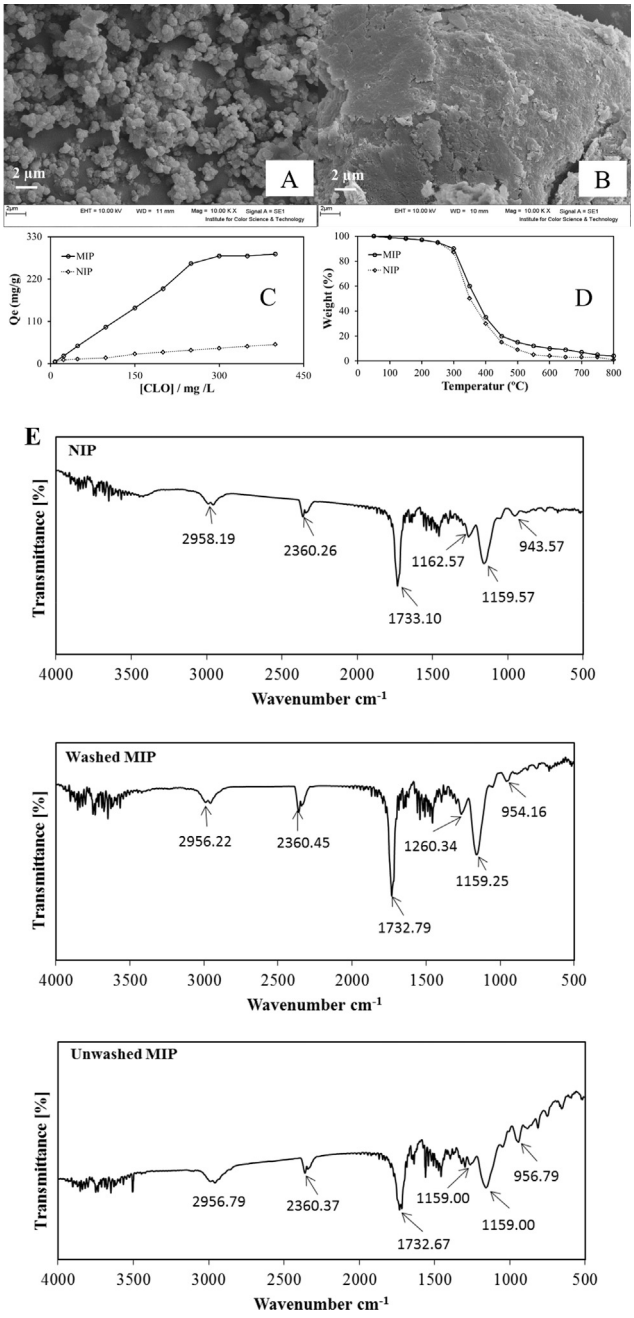

Fig. 1. The SEM imaging representing morphologies of (A) NIP and (B) MIP. Magnification 10K×. The comparison of adsorption capacity the NIP and MIP toward CLO. (Conditions: pH = 8.5, 0.79 g MIP and 89 min as contact time (C). The thermogravimetric analysis of MIPs and NIPs (D). The FT-IR spectra of NIP and MIPs before and after washing CLO (E).

removal in optimal conditions at various concentrations of CLO was investigated, the results are presented in Fig. 1c. Regarding the graph, it can be seen that the polymer capacity of MIP increased with increasing CLO concentration.

Table 1 summarizes data of the N_2 adsorption and desorption analysis on MIP and NIP particles. As shown in the table, the specific surface area, total pore volume and pore size for MIP are 18.11 cm^2/g, 0.52 cm^3/g and 42.91 nm, respectively. By comparing the values of the specific surface, it is confirmed that the imprinting in the polymers is well done.

The FT-IR spectra of the synthesized MIPs and NIPs were obtained in the range of 500–4000 cm^{-1} by Bruker Tensor 27 FTIR

Table 1
Data analysis from N_2 adsorption–desorption Isotherm.

Sorbent	Special surface area (cm^2/g)	Total pores volumes (cm^3/g)	Average of pores sizes (nm)
MIP	18.11	0.52	42.91
NIP	12.43	0.24	40.45

Spectrometer. Fig. 1E shows FT-IR spectra of CLO-MIP after and before removing the template (washed and unwashed, respectively) and NIP. It can be seen that the spectrum of MIPs and NIP are similar, indicating similarity in the structure of the network. There is a broad band between 1100 and 1200 cm^{-1}, corresponding to the stretching vibrations of –C–O–C– that could be attributed to the link of the MAA monomer and cross-linker EGDMA.

In addition, there are absorptions due to a stretch of the carbonyl group (1733 cm^{-1}), C—O stretch (1263 cm^{-1}), and vibration C—H (756, 1396, 1458 and 2962 cm^{-1}). At 2995 and 2962 cm^{-1}, are the stretching vibrations of C—H, band at 1458 cm^{-1} appears to be due to $-CH_2-$, and the band in 1398 cm^{-1} may be due to CH_3. The sharp peak at 1733 cm^{-1} is the characteristic peak of C═O stretch, due to C═O vibration of EGDMA. Likewise, it was also identified similarities between the spectrum of the template and MIP unwashed mainly in the C—N and C—C bonds (500–1600 cm^{-1}). After washing, the spectra of the MIP are comparable to the NIP (blank polymer), which indicates that the entire template was removed from the MIP unwashed. At the FT-IR spectrum of MIP unwashed, there are two clear absorptions at 3500 and 1560 cm^{-1} related to O—H stretch and N—H stretching, respectively. The presence of these peaks can be attributed to the interaction between the hydrogen of the carbonyl groups as well as nitrogen groups of the CLO with the functional groups of MAA. Similar results were obtained by Soledad-Rodríguez et al. [16], they were synthesized MIPs based in MAA as monomer and EGDMA as cross-linker, found in general, that the FT-IR spectra for all the MIPs are very similar each to other, consistent with the fact that all the products were synthesized based on same monomer and cross-linker, and also there was no significant difference between MIPs and NIPs.

The N_2 adsorption-desorption curves for MIP and NIP particles was plotted in Sup Fig. 3. As can be seen, N_2 absorption curve of the MIP particle did not overlap on the desorption curve, unlike absorption- desorption curve of NIP particles. In addition, Table 1 summarizes data of the N2 adsorption and desorption analysis on MIP and NIP particles. The results of N2 adsorption-desorption isotherms for MIP and NIP particles are represented in the Sup Fig 4.

The thermogravimetric analysis (TGA) curves of the MIPs and NIPs are given in Fig. 1d. It can be seen with the temperature increase at the range of 250–600 °C, the weight of both polymers was significantly decreased due to thermal decomposition the residual organic substrate. There existed about 6.34% difference in the weight retention between NIP and MIPs. This small difference in weight retention could be owing to the residual template molecules in MIPs.

3.2. Evaluation of the separation capacity and selectivity

The maximum absorption capacity (q) of MIP particles was determined to 280 mg/g. However, the maximum NIP capacity was 40 mg/g. These results confirm that MIP has a high ability to absorb CLO. It is likely that low-absorbed amounts on the NIP are also due to poor physical interactions between CLO and polymer particles. In the removal of CLO by modified silica particles, researchers have reported that the maximum absorption capacity by particles is 6.5 mg/g of absorbent [41]. In another study, the authors reported that one gram of synthesized MIP particles for ampicillin can absorb 13.5 mg of antibiotics [42]. Compared to these cases, the polymer particles prepared in this study are much more efficient.

High selectivity is one of the most important characteristics of MIPs to the template molecule. This is probably due to the fact that, during molecular imprinting, the functional groups of the template molecules (here CLO) form a unique arrangement toward the functional groups of monomer units, which is specific to itself. In order to verify the selectivity of MIPs toward CLO, other □-lactam antibiotics with similar chemical structures as competitive molecules: Amoxicillin (AMOX), Oxacillin (OXA), and Penicillin G (PEN-G) were examined (see Sup Fig. 3). For interference studies, recoveries of these antibiotics at concentration levels of 1 μM were tested by a procedure developed for the MIPs. These results demonstrated that the synthesized MIP particles for CLO exhibited specific selectivity towards CLO in the presence of other structurally related compounds, as they are shown in the Sup Fig. 1.

3.3. Characterization of nanomaterials and modified electrode

The TEM image, Fig. 2a, is representing the appropriate conditions of single layer GO and the image of the purchased AuNPs (Fig. 2b) is representing the correct shape and size and also lack of agglomeration. Furthermore, the FE-SEM images of the nanomaterials-modified working area of the SPCEs was shown the correct assembly and decoration of the nanomaterials. Fig. 2c, shows a single layer of the GO on the bare SPCE is shown while in the image of Fig. 2d, the decoration of the AuNPs on the GO-modified SPCE are characterized. This observation suggests that AuNPs/GO nano composition has been prepared properly. Furthermore, the Energy Dispersive Spectroscopy (EDS) analysis (Fig. 2e) shows the elemental composition of the modified electrode and as it can be seen the carbon, oxygen and gold are the main components. This is another evidence that the nanocomposite of graphene oxide and gold nanoparticles are forming the surface of the modified electrode, to be used as the designed electrochemical nanosensor.

The Cyclic Voltammetry (CV) and Electrochemical Impedance Spectroscopy (EIS) as reliable electrochemical characterization methods were performed to assess the modification steps of the working electrode. The cyclic voltammograms of the modified electrodes were recorded in a 0.1 M phosphate buffer containing 5.0 mM $K_3[Fe(CN)_6]$ at pH 7 and shown in Fig. 3a.

The oxidation peak intensity decreased at the surface of the electrode after the modification of SPCE with GO, in comparison to the bare SPCE. This can be interpreted in that GO has a partially negative charge, and $K_3[Fe(CN)_6]$ in an aqueous environment has a negative charge too. The presence of $K_3[Fe(CN)_6]$ reduced at the surface of the GO/SPCE due to the repulsion among the same charges. It can be seen that the oxidation current of $K_3[Fe(CN)_6]$ was increased due to the presence of AuNPs at the SPCE surface modified with GO. Due to its high conductivity, partially positive charge and very small dimensions, AuNPs increased the effective surface area of the electrode and the sensitivity of the sensor to $K_3[Fe(CN)_6]$. This observation suggests that the AuNPs/GO hybrid is a promising material that can improve the electrochemical sensitivity of electrodes for $K_3[Fe(CN)_6]$ detection.

In the EIS studies, the Nyquist curves consisting of the imaginary part of the impedance versus the actual part at each frequency in a solution of 5.0 mM $K_3[Fe(CN)_6]$ containing 1.0 M KCl for various electrodes, showed in the Fig. 3b. In EIS, upon modification of the SPCE with GO, the R_{ct} significantly increased. This could be due to the insulating nature of the GO [33]. As the SPCE surface was is modified with AuNPs, the electrode showed lower resistance. This is because AuNPs has a large surface area and good conductivity, and the slope of the linear region that represents the

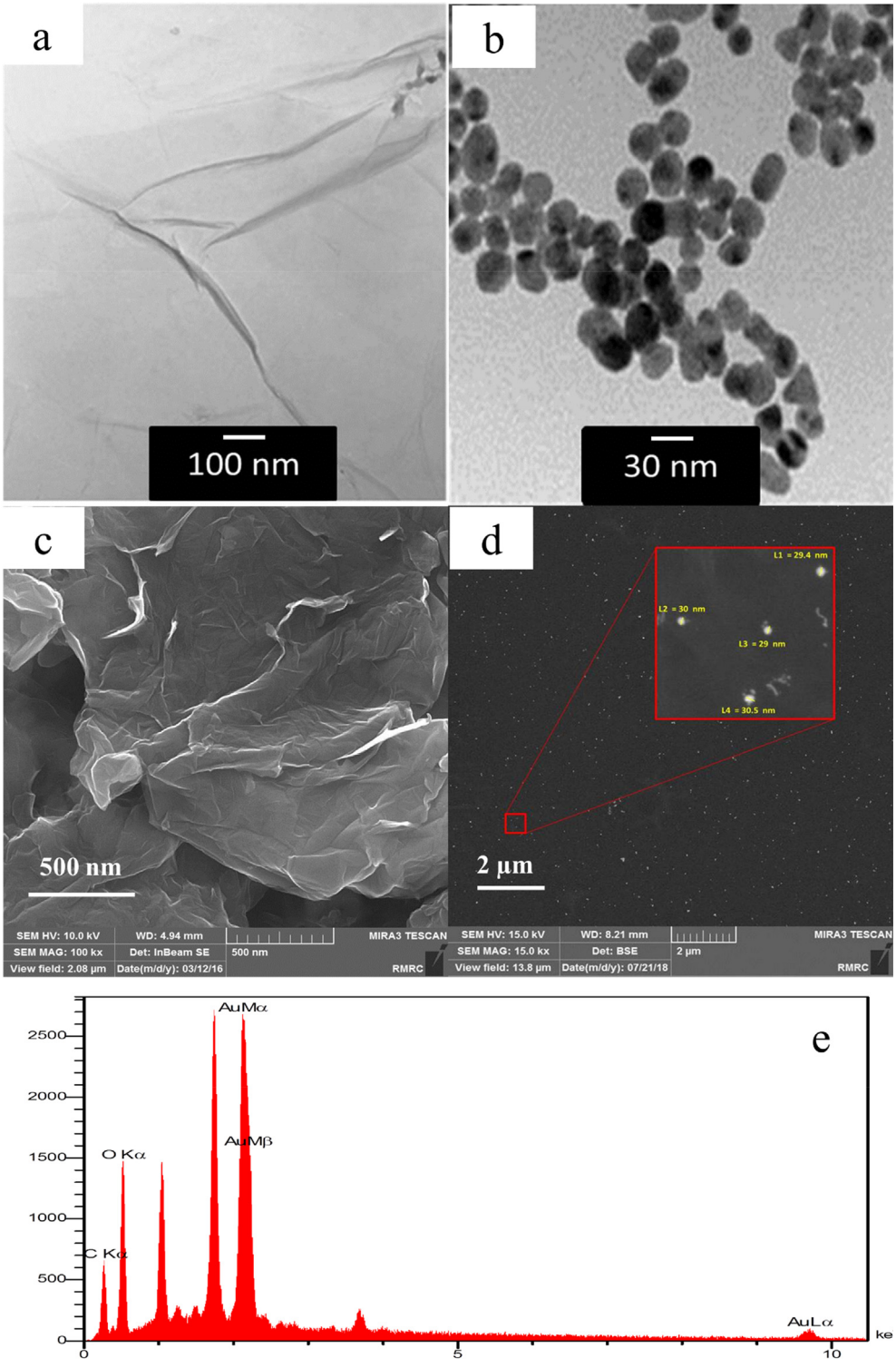

Fig. 2. The TEM images of the Graphene Oxide (GO) (a) and the Gold Nanoparticles (b). The FE-SEM images of the GO-modified SPCE electrode (c), GO/AuNPs-modified SPCE electrode (d) and EDX of the GO/AuNPs-modified SPCE electrode (e).

surface diffusion control process is has increased. It can be concluded that the behavior of the modified electrode is in agree in both CV and EIS studies.

3.4. Electrochemical detection of CLO in buffer and milk samples

In order to determine of CLO in solution, a calibration curve is first required to measure the concentration CLO in samples. The calibration curve was plotted based on the electrochemical sensor response of AuNPs/GO SPCE towards different concentrations of CLO, as shown in Fig. 3c. As shown in this Figure, the oxidation peak current is increased by the gradual increase of CLO concentration, and there is a direct linear relationship between the concentration and the oxidation peak current, as shown in Fig. 3d. The residues CLO concentration at any time of the collection process was calculated based on the peak-oxidation current and using the equation shown in Fig. 3d. The wide linear range from 110 nM to 750 nM and the detection limit of 36 nM describes a

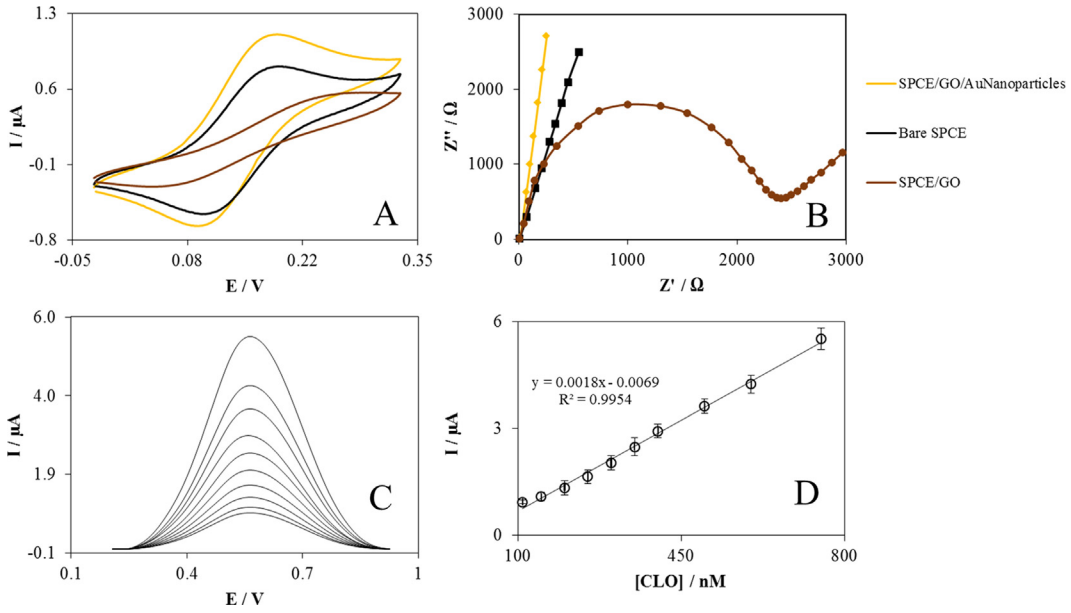

Fig. 3. The cyclic voltammetry (CV) of the different modified electrode in the 1.0 mM $K_3[Fe(CN)_6]$ solution in phosphate buffer solution (a) and the Nyquist plot of the different electrodes in the solution of 5.0 mM $K_3[Fe(CN)6]$ containing 1.0 M KCl (b). Differential pulse voltammetry of modified screen-printed carbon electrode with Au nanoparticles and graphene oxide in buffer phosphate solution (pH 7.0) containing different CLO concentration. Numbers 1–10 represents CLO concentration range in 110–750 nM (C). The calibration curve of CLO sensor (D).

sensitive detection method of CLO comparing to previous similar publications in this field [43–48]. This might be because of applied graphene oxide and gold nanoparticles for electrode modification that expand the surface area and also accelerate electron transfer as well as the electrocatalytic effect of gold nanoparticles. Another reason could be the use of MIP for pre-concentration of the CLO molecules prior to being quantified using developed electrochemical nanosensor. In another experiment, the repeatability of the nanosensor was assessed by 12 replications of the sensor fabrication process and the relative standard deviation was 4.6% which is very acceptable.

In addition, the nanosensor has tested for stability in 7 days after fabrication and the stability was 91.1% compared to the freshly fabricated biosensor. The repeatability of the nanosensor was also tested by the nanosensor in 5 replication and relative standard deviation of replications was 6.1% which is in acceptable order.

Additionally, in order to evaluate the performance of synthesized MIP particles for absorbing residues CLO values in real samples such as milk, 0.79 g of MIP particles were added to 20 mL of milk, which prepared from a livestock farm in Yazd, after stirring of solution for 89 min, polymer particles were removed from the milk using a paper filter. The concentration of CLO in the milk was calculated before and after the addition of MIP particles by electrochemical nanosensor that discussed earlier, and the average value of 10 replicates was reported in Table 2. To confirm the measurement method and high adsorption capability, different volumes of CLO with given concentration were added to the milk. The results of this test indicate the proper performance of MIP adsorbent particles in the effective collection of the antibiotic residues of CLO from aqueous media that could be used for pre-concentration of the CLO and determined afterward using a simple developed electrochemical nanosensor.

Table 2
Results of CLO Measurement in milk sample.

Added (nM)	Found (nM)	Recovery (%)	Relative standard deviation (%)
150.0	152.8	101.8	5.3
250.0	246.7	98.6	4.6
500.0	501.5	100.3	4.3

4. Conclusions

This research focused on the evaluation of MIPs as a sorbent for the selective recognition and adsorption for CLO to pre-concentrate. The maximum CLO adsorption capacity on MIP adsorbent in the optimum conditions, including pH, 8.5 and contact time of 89 min, is 280 mg/g. The adsorption selectivity experiments suggested that the MIPs exhibited high affinity toward CLO when compared with NIPs, even in the presence of other compounds. This high capacity indicates that synthesized MIP particles can be used to effectively reduce the residue of drug contamination in dairy samples. The developed electrochemical nanosensor showed a good electrocatalytic activity towards CLO and the high sensitivity for CLO detection were of advantages of this method. Finally, the good function of both pre-concentration and electrochemical detection of the CLO in a real sample of milk could be a new way to determine the residual dosage of the CLO antibiotic in dairy products to avoid consequences of excessive consumption of the antibiotic in human foods.

Acknowledgment

Authors are grateful to colleagues of Research Center the Polymer and Textile, Islamic Azad University of Yazd.

Declaration of Competing Interest

The authors have declared no conflict of interest.

Appendix A. Supplementary data

Supplementary data to this article can be found online at https://doi.org/10.1016/j.measurement.2019.05.068.

References

[1] J. Jeong, W. Song, W.J. Cooper, J. Jung, J. Greaves, Degradation of tetracycline antibiotics: mechanisms and kinetic studies for advanced oxidation/reduction processes, Chemosphere 78 (2010) 533–540.
[2] M. NooriSepehr, S. Mohebi, S. AbdlollahiVahed, M. Zarrabi, Removal of tetracycline from synthetic solution by natural LECA, J. Environ. Health Eng. 1 (2014) 301–311.
[3] E.S. Elmolla, M. Chaudhuri, The feasibility of using combined TiO2 photocatalysis-SBR process for antibiotic wastewater treatment, Desalination 272 (2011) 218–224.
[4] E.A. Serna-Galvis, A.L. Giraldo-Aguirre, J. Silva-Agredo, O.A. Flórez-Acosta, R.A. Torres-Palma, Removal of antibiotic cloxacillin by means of electrochemical oxidation, TiO2 photocatalysis, and photo-Fenton processes: analysis of degradation pathways and effect of the water matrix on the elimination of antimicrobial activity, Environ. Sci. Pollut. Res. 24 (2017) 6339–6352.
[5] W. Du, M. Sun, P. Guo, C. Chang, Q. Fu, Molecularly imprinted membrane extraction combined with high-performance liquid chromatography for selective analysis of cloxacillin from shrimp samples, Food Chem. 259 (2018) 73–80.
[6] J.Y. Song, B.N. Bhadra, S.H. Jhung, Contribution of H-bond in adsorptive removal of pharmaceutical and personal care products from water using oxidized activated carbon, Microporous Mesoporous Mater. 243 (2017) 221–228.
[7] X. Wang, J. Zhang, V.W. Chang, Q. She, C.Y. Tang, Removal of cytostatic drugs from wastewater by an anaerobic osmotic membrane bioreactor, Chem. Eng. J. 339 (2018) 153–161.
[8] Y. Chen, F. Wang, L. Duan, H. Yang, J. Gao, Tetracycline adsorption onto rice husk ash, an agricultural waste: its kinetic and thermodynamic studies, J. Mol. Liq. 222 (2016) 487–494.
[9] P. Nebout, B. Cagnon, S. Delpeux, A. Di Giusto, O. Chedeville, Comparison of the efficiency of adsorption, ozonation, and ozone/activated carbon coupling for the removal of pharmaceuticals from water, J. Environ. Eng. 142 (2015) 04015074.
[10] S. Cherif, M. Boudraa, A. Moussa, R. Maachi, N. Nasrallah, N. Guendouz, Degradation of a pharmaceutical pollutant by coupling photo-fenton and adsorption processes, in: International Symposium on Materials and Sustainable Development, Springer, 2017, pp. 580–592.
[11] P. Zeng, J. Du, Y. Song, Y. Liu, R. Liu, P. Zhang, S. Xiao, Efficiency comparison for treatment of amantadine pharmaceutical wastewater by Fenton, ultrasonic, and Fenton/ultrasonic processes, Environ. Earth Sci. 73 (2015) 4979–4987.
[12] A. Almasi, A. Dargahi, M. Mohamadi, H. Biglari, F. Amirian, M. Raei, Removal of Penicillin G by combination of sonolysis and Photocatalytic (sonophotocatalytic) process from aqueous solution: process optimization using RSM (Response Surface Methodology), Electron. Phys. 8 (2016) 2878.
[13] Z. Frontistis, Degradation of the nonsteroidal anti-inflammatory drug piroxicam from environmental matrices with UV-activated persulfate, J. Photochem. Photobiol., A (2019).
[14] A. Carmalin Sophia, E.C. Lima, N. Allaudeen, S. Rajan, Application of graphene based materials for adsorption of pharmaceutical traces from water and wastewater-a review, Desalin. Water Treat. 57 (2016) 27573–27586.
[15] M.H. Khan, H. Bae, J.-Y. Jung, Tetracycline degradation by ozonation in the aqueous phase: proposed degradation intermediates and pathway, J. Hazard. Mater. 181 (2010) 659–665.
[16] I.R. Bautitz, R.F.P. Nogueira, Degradation of tetracycline by photo-Fenton process—solar irradiation and matrix effects, J. Photochem. Photobiol., A 187 (2007) 33–39.
[17] A.H. Mahvi, A. Maleki, Photosonochemical degradation of phenol in water, Desalin. Water Treat. 20 (2010) 197–202.
[18] A. Mahvi, A. Maleki, R. Rezaee, M. Safari, Reduction of humic substances in water by application of ultrasound waves and ultraviolet irradiation, Iranian J. Environ. Health Sci. Eng. 6 (2009) 233–240.
[19] P. NaVrátiloVá, Screening methods used for the detection of veterinary drug residues in raw cow milk–a review, Czech J. Food Sci. 26 (2008) 393–401.
[20] D. Davoodi, M. Hassanzadeh-Khayyat, M.A. Rezaei, S.A. Mohajeri, Preparation, evaluation and application of diazinon imprinted polymers as the sorbent in molecularly imprinted solid-phase extraction and liquid chromatography analysis in cucumber and aqueous samples, Food Chem. 158 (2014) 421–428.
[21] S. Shojaei, N. Nasirizadeh, M. Entezam, M. Koosha, M. Azimzadeh, An electrochemical nanosensor based on molecularly imprinted polymer (MIP) for detection of gallic acid in fruit juices, Food Anal. Methods 9 (2016) 2721–2731.
[22] S. Jafari, M. Dehghani, N. Nasirizadeh, M. Azimzadeh, An azithromycin electrochemical sensor based on an aniline MIP film electropolymerized on a gold nano urchins/graphene oxide modified glassy carbon electrode, J. Electroanal. Chem. 829 (2018) 27–34.
[23] J. Ashley, K. Wu, M.F. Hansen, M.S. Schmidt, A. Boisen, Y. Sun, Quantitative detection of trace level cloxacillin in food samples using magnetic molecularly imprinted polymer extraction and surface-enhanced Raman spectroscopy nanopillars, Anal. Chem. 89 (2017) 11484–11490.
[24] K. Du, Z. Luo, P. Guo, W. Tang, N. Wu, P. Zheng, W. Du, A. Zeng, W. Jing, C. Chang, Preparation and evaluation of a molecularly imprinted sol–gel material as the solid-phase extraction adsorbents for the specific recognition of cloxacilloic acid in cloxacillin, J. Sep. Sci. 39 (2016) 483–489.
[25] S.N. Topkaya, M. Azimzadeh, M. Ozsoz, Electrochemical biosensors for cancer biomarkers detection: recent advances and challenges, Electroanalysis (2016) n/a-n/a.
[26] S.M. Seifati, N. Nasirizadeh, M. Azimzadeh, Nano-biosensor based on reduced graphene oxide and gold nanoparticles, for detection of phenylketonuria-associated DNA mutation, IET Nanobiotechnol. 12 (2017) 417–422.
[27] A. Khodadadi, E. Faghih-Mirzaei, H. Karimi-Maleh, A. Abbaspourrad, S. Agarwal, V.K. Gupta, A new epirubicin biosensor based on amplifying DNA interactions with polypyrrole and nitrogen-doped reduced graphene: experimental and docking theoretical investigations, Sens. Actuators B 284 (2019) 568–574.
[28] Y. Akbarian, M. Shabani-Nooshabadi, H. Karimi-Maleh, Fabrication of a new electrocatalytic sensor for determination of diclofenac, morphine and mefenamic acid using synergic effect of NiO-SWCNT and 2, 4-dimethyl-N/-[1-(2, 3-dihydroxy phenyl) methylidene] aniline, Sens. Actuators B 273 (2018) 228–233.
[29] M. Azimzadeh, N. Nasirizadeh, M. Rahaie, H. Naderi-Manesh, Early detection of Alzheimer's disease using a biosensor based on electrochemically-reduced graphene oxide and gold nanowires for the quantification of serum microRNA-137, RSC Adv. 7 (2017) 55709–55719.
[30] M. Miraki, H. Karimi-Maleh, M.A. Taher, S. Cheraghi, F. Karimi, S. Agarwal, V.K. Gupta, Voltammetric amplified platform based on ionic liquid/NiO nanocomposite for determination of benserazide and levodopa, J. Mol. Liq. 278 (2019) 672–676.
[31] S. Cheraghi, M.A. Taher, H. Karimi-Maleh, Highly sensitive square wave voltammetric sensor employing CdO/SWCNTs and room temperature ionic liquid for analysis of vanillin and folic acid in food samples, J. Food Compos. Anal. 62 (2017) 254–259.
[32] Y. Shao, J. Wang, H. Wu, J. Liu, I.A. Aksay, Y. Lin, Graphene based electrochemical sensors and biosensors: a review, Electroanalysis 22 (2010) 1027–1036.
[33] M. Azimzadeh, M. Rahaie, N. Nasirizadeh, K. Ashtari, H. Naderi-Manesh, An electrochemical nanobiosensor for plasma miRNA-155, based on graphene oxide and gold nanorod, for early detection of breast cancer, Biosens. Bioelectron. 77 (2016) 99–106.
[34] M. Ho Yang, B.G. Choi, H. Park, T.J. Park, W.H. Hong, S.Y. Lee, Directed self-assembly of gold nanoparticles on graphene-ionic liquid hybrid for enhancing electrocatalytic activity, Electroanalysis 23 (2011) 850–857.
[35] J.H. Shim, J. Kim, C. Lee, Y. Lee, Electrocatalytic activity of gold and gold nanoparticles improved by electrochemical pretreatment, J. Phys. Chem. C 115 (2010) 305–309.
[36] M. Pumera, Graphene in biosensing, Mater. Today 14 (2011) 308–315.
[37] S.N. Topkaya, M. Azimzadeh, Biosensors of in vitro detection of cancer and bacterial cells, in: Nanobiosensors for Personalized and Onsite Biomedical Diagnosis, Institution of Engineering and Technology, 2016, pp. 73–94.
[38] S. Jafari, N. Nasirizadeh, M. Dehghani, Developing a highly sensitive electrochemical sensor using thiourea-imprinted polymers based on an MWCNT modified carbon ceramic electrode, J. Electroanal. Chem. 802 (2017) 139–146.
[39] T. Esfandiyari, N. Nasirizadeh, M. Dehghani, M.H. Ehrampoosh, Graphene oxide based carbon composite as adsorbent for Hg removal: preparation, characterization, kinetics and isotherm studies, Chin. J. Chem. Eng. 25 (2017) 1170–1175.
[40] Z. Li, L. Schulz, C. Ackley, N. Fenske, Adsorption of tetracycline on kaolinite with pH-dependent surface charges, J. Colloid Interface Sci. 351 (2010) 254–260.
[41] B. Soledad-Rodriguez, P. Fernandez-Hernando, R. Garcinuno-Martinez, J. Durand-Alegria, Effective determination of ampicillin in cow milk using a molecularly imprinted polymer as sorbent for sample preconcentration, Food Chem. 224 (2017) 432–438.
[42] N. Wu, Z. Luo, Y. Ge, P. Guo, K. Du, W. Tang, W. Du, A. Zeng, C. Chang, Q. Fu, A novel surface molecularly imprinted polymer as the solid-phase extraction adsorbent for the selective determination of ampicillin sodium in milk and blood samples, J. Pharm. Anal. 6 (2016) 157–164.
[43] L.R. Schoukroun-Barnes, S. Wagan, R.J. White, Enhancing the analytical performance of electrochemical RNA aptamer-based sensors for sensitive detection of aminoglycoside antibiotics, Anal. Chem. 86 (2014) 1131–1137.
[44] E. Zacco, J. Adrián, R. Galve, M.-P. Marco, S. Alegret, M.I. Pividori, Electrochemical magneto immunosensing of antibiotic residues in milk, Biosens. Bioelectron. 22 (2007) 2184–2191.
[45] A.A. Rowe, E.A. Miller, K.W. Plaxco, Reagentless measurement of aminoglycoside antibiotics in blood serum via an electrochemical, ribonucleic acid aptamer-based biosensor, Anal. Chem. 82 (2010) 7090–7095.
[46] G.E. Pellegrini, G. Carpico, E. Coni, Electrochemical sensor for the detection and presumptive identification of quinolone and tetracycline residues in milk, Anal. Chim. Acta 520 (2004) 13–18.
[47] Z.-G. Yu, R.Y. Lai, A reagentless and reusable electrochemical aptamer-based sensor for rapid detection of ampicillin in complex samples, Talanta 176 (2018) 619–624.
[48] K. Ghanbari, M. Roushani, A novel electrochemical aptasensor for highly sensitive and quantitative detection of the streptomycin antibiotic, Bioelectrochemistry 120 (2018) 43–48.